NATIONAL ADVISORY COMMITTEE FOR AERONAUTICS

TECHNICAL NOTE 3995

AN INVESTIGATION OF FLOW IN CIRCULAR AND ANNULAR

90° BENDS WITH A TRANSITION IN CROSS SECTION

By Stafford W. Wilbur

Langley Aeronautical Laboratory
Langley Field, Va.

NACA

Washington

August 1957

NATIONAL ADVISORY COMMITTEE FOR AERONAUTICS

TECHNICAL NOTE 3995

AN INVESTIGATION OF FLOW IN CIRCULAR AND ANNULAR

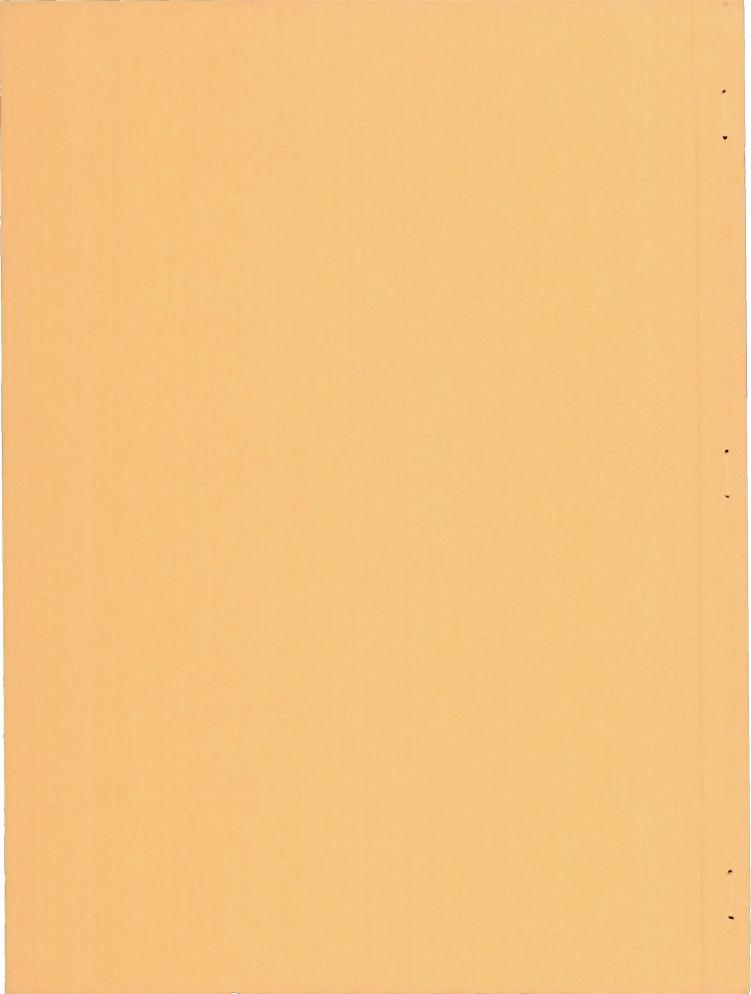90° BENDS WITH A TRANSITION IN CROSS SECTION

By Stafford W. Wilbur

SUMMARY

An investigation at low speed of the performances of circular and annular 90° bends of simple shapes was conducted for configurations for which the cross-sectional area was constant, expanding, and contracting. Two series of transition bends (circular to annular and annular to circular) were included, in which the transition occurred upstream of the bend, within the bend, and downstream from the bend. The data presented include the exit velocity profiles, the relative total-pressure-loss coefficients measured at the exit station, and an index for the exit total-pressure distortion. Separation of the flow in the bend occurred for all configurations except those with a contracting area. With the transition in cross section downstream of the bend proper, the separated region was removed by natural mixing but was accompanied by high pressure losses. Certain locations of the transition produced higher performances than others.

INTRODUCTION

Much research has been undertaken in an effort to obtain a better understanding of the flow of fluids through bends. Most of this research has been done with bends of constant-cross-section shape, and summaries of existing data on this type of 90° bend can be obtained in references 1 and 2. Reference 3 presents the high-speed performance of this type of bend. With the advent of the turbojet and ram-jet engines, more emphasis has, of necessity, been placed on the more unconventional type of bends that may be incorporated into the internal flow systems of such engines. Quite frequently, it is desired to admit air at the wing root, or through a scoop, after which the air must pass by means of a bend system to the engine intake located in the body of the aircraft. The losses and the distortion of the velocity distribution at the entrance to the jet engine must be kept small.

The purpose of the present investigation was to determine with a minimum of measurements the performances of 90° bends with various combinations of cross-section transition (circular to annular and annular to circular) in order to evaluate any general advantages of one design over another. The principal data used to determine performance were exit velocity and total-pressure distributions and tuft observations throughout the bends. Brief investigations of the effect of area change in circular and annular bends are also included. The inlet Mach number was approximately 0.2 for all configurations except the reducing bends; these had an inlet Mach number of 0.1.

SYMBOLS

A   cross-sectional area

d   diameter

D   diameter of circle of same area as bend-cross-section flow area

p_t total pressure

p   static pressure

q_c impact pressure, $p_t - p$

r   radius from duct center line to point in stream

r_c mean radius of curvature of bend

R   radius from duct center line to duct wall

u   local velocity

U   reference inlet velocity, based on $p_{t,r}$ and average wall static pressure at inlet station

l inlet approach length

G   flow-distortion index, $\displaystyle\int \frac{\Delta p_t}{q_{c,r}} \frac{dA}{A}$

Δp_t loss in total pressure between reference pressure $p_{t,r}$ and point in exit station survey

Subscripts:

r   reference conditions

i   inner body

o   outer body

A bar over a symbol indicates a weighted value.

APPARATUS, TESTS, AND METHODS

General Arrangement

The apparatus for this investigation consists of the particular bend under consideration preceded by an inlet duct of constant area, an inlet bell, and a 54-inch-diameter duct which was connected to a centrifugal compressor. Downstream of the bend was a uniform cross-section duct through which the air passed before being discharged into the surrounding atmosphere. The outer wall of the bend was formed from transparent plastic reinforced with mahogany; the inner bodies in the bend were constructed from mahogany. The remaining ducts were made of steel. A photograph of a typical bend (configuration 8) is presented as figure 1. Diagrams of the various bend configurations investigated are shown in figure 2.

The bends investigated were of five general categories. Dimensions of bend sections having other than circular-arc curvature may be obtained from table I. Throughout the rest of this report, the various configurations are identified as follows:

(a) Constant-area, constant-cross-section bends (fig. 2(a))

         Configuration 1 - circular ($r_c/D = 1.00$)
         Configuration 2 - annular ($r_c/D = 1.38$)

(b) Constant-area transition bends with cross section changing from circular to annular (fig. 2(b))

         Configuration 3 - change in cross-section shape occurs before bend proper ($r_c/D = 1.38$)

         Configuration 4 - change in cross-section shape occurs within bend proper ($r_c/D = 1.38$)

         Configuration 5 - change in cross-section shape occurs after bend proper ($r_c/D = 1.00$)

(c)   Constant-area transition bends with cross section changing from
       annular to circular (fig. 2(c))

>   Configuration 6 - change in cross-section shape occurs
>   before bend proper ($r_c/D = 1.00$)
>   Configuration 7 - change in cross-section shape occurs
>   within bend proper ($r_c/D = 1.38$)
>   Configuration 8 - change in cross-section shape occurs
>   after bend proper ($r_c/D = 1.38$)

(d)   Diffusing bends (fig. 2(d))

>   Configuration 9 - circular; area ratio = 1.9
>   Configuration 10 - change from annular to circular cross-
>   section shape occurs within bend; area ratio = 1.9

(e)   Reducing bends (fig. 2(e))

>   Configuration 11 - circular; area ratio = 0.526
>   Configuration 12 - change from circular to annular cross-
>   section shape occurs within bend; area ratio = 0.526

Instrumentation

A ring of four equispaced static-pressure orifices was located at
both the inlet and the exit stations of the bend. (See fig. 2(f).) Two
pitot-static-pressure survey rakes were mounted at the inlet in the plane
of symmetry; at the exit survey station two pitot-static-pressure survey
rakes were mounted in the plane of symmetry and one pitot-static-pressure
survey rake was mounted normal to the plane of symmetry.

Tufts of cotton yarn attached with adhesive cellophane tape were
equally spaced throughout the bends to indicate the character of the flow
near the walls. Exit pressure surveys were made both with and without
tufts to determine the effect of tufts on the flow.

Tests and Methods

All tests were made at low speeds with Mach numbers ranging between
0.1 and 0.2 and Reynolds numbers (based on duct hydraulic diameter) varying
from 0.68×10^6 to 2.2×10^6. Inlet pressure surveys were made in order
to determine the general nature and thickness of the boundary layer and
to determine the flow asymmetry in the plane of measurement. Inlet
boundary-layer flow was turbulent in all cases. Tuft studies were made
to determine the general flow patterns throughout the bends.

Exit pressure surveys (with and without tufts) were made to determine the exit velocity and total-pressure distributions and the mean total-pressure-loss coefficient $\frac{\overline{\Delta p_t}}{q_{c,r}}$. The impact pressure $q_{c,r}$ is defined as $p_{t,r}$ minus the arithmetic average of the four wall static-pressure measurements at the inlet survey station. For cases in which attached flow was obtained at all survey positions at the bend exit, the bend loss coefficient was obtained by mass weighting the three exit total-pressure surveys. The assumptions were made that each survey covered one-fourth of the exit area and that the total-pressure distributions were the same at the top and at the bottom of the bend exit. For cases in which separated flow was present at the exit downstream from the inner part of the bend, a modified loss-coefficient evaluation was used. In these cases, the weighted total-pressure loss of the flow in the inner 25 percent of the exit cross section was added to the theoretical loss required to mix the nonuniform distribution of that portion of the flow to a uniform one in a constant-area frictionless duct. The theoretical loss was evaluated by use of the "mass-momentum" method of reference 4, which assumes conservation of momentum and maintenance of continuity. The use of this procedure allowed the final mean loss coefficient for the separated-flow cases to be based on the same type of exit flow distribution as that for the attached-flow cases; thus, all the data were made comparable. The total-pressure distribution downstream from the inner part of the bend for either the attached-flow cases or the modified separated-flow cases was uniform radially; however, the total-pressure level was appreciably below that for the other survey locations. The loss coefficient based on a perfectly uniform downstream distribution would be somewhat higher than those presented herein.

In order to obtain an index reflecting the magnitude and extent of the exit total-pressure distortion, the measured point values of loss coefficient were area weighted to obtain an average value. Surveys which indicated essentially no total-pressure loss except a moderate amount of boundary layer at the walls were not included in the distortion index. The significant difference between mass-weighted and area-weighted mean-loss-coefficient values is that a mass-weighted value is not materially affected by large areas of separation since no flow exists in these regions, whereas an area-weighted value would be significantly increased by the existence of such regions.

RESULTS AND DISCUSSION

Inlet Velocity Profiles

All the inlet velocity profiles correspond to relatively thin inlet boundary layers. (See fig. 3.) The impact pressure ratios indicated by

table II correspond to Mach numbers between 0.1 and 0.21.   The profiles show that the flow in the plane of the inlet survey measurements was influenced by the configuration at and immediately downstream of the inlet station, primarily by transverse static-pressure gradients set up by the bends and by the center-body design.   Configurations 3 and 6 had an area-transition section between the inlet and the bend proper.   This transition was responsible for more symmetrical inlet velocity distributions since the survey was upstream of the transverse static-pressure gradients associated with the bend.   The remaining configurations had similar inlet velocity distributions.   The local-flow acceleration which occurred on the inner wall of the bend was responsible for increased velocities at the inlet station in the region of the inner wall.

Exit Velocity and Total-Pressure Profiles

Both of the constant-area, constant-cross-section bends (circular and annular) had separation on the bend inner wall at the exit survey station (configurations 1 and 2, fig. 4(a)).   The measurements at the exit indicate fairly uniform distributions except in the immediate region of separation.   The constant-area, circular-cross-section bend gives exit velocity profiles that are in close agreement with references 3 and 5. The present configuration had an inlet-duct length equivalent to one-seventh of that of reference 5.   Reference 3 shows that there is a very slight effect on the flow at the exit of a 90° bend due to changing the inlet displacement thickness.

Although both annular- and circular-cross-section bends resulted in a similar type of exit velocity profile, the circular bend had a shorter inlet-duct length (0.667 hydraulic diameter) as compared with that for the annular bend (2.15 hydraulic diameters).   This difference in length would be offset, at least in part, by the larger effective radius ratio of the annular bend ($r_c/D = 1.38$ as compared with $r_c/D = 1.00$ for the circular bend).   References 1 to 3 indicate that for the ranges of the present report the radius ratio of the bend has a considerably greater influence over the loss coefficient than does the inlet-duct length. Since exit-pressure survey data for 90° annular bends are limited, the true effect of radius ratio is unknown for this type.   However, the exit velocity distribution of the annular bend (configuration 2) is about comparable to that for a circular bend with r_c/D of 1.5.   (See ref. 6.) This result suggests that, for constant-area, constant-cross-section bends, the ratio of the radius of curvature to the diameter of a circle with the same cross-sectional area as the bend is a close correlating parameter.

Exit velocity profiles for constant-area transition bends with cross section changing from circular to annular (configurations 3, 4, and 5) are given in figure 4(b). The data indicate that separation occurs on the bend inner wall of configurations 3 and 4, whereas no separation occurs at the exit station of configuration 5. Since the duct-cross-section transition occurred downstream of the bend for configuration 5, the separated bend flow evidenced by tufts mixed and reattached before the exit survey plane was reached. The magnitude of the effect of the transition section on the flow distribution may be obtained by comparing profiles for configurations 1 and 5. A comparison of the velocity distributions of configurations 3 and 4 with that of configuration 2 (fig. 4 (a)) indicates a close similarity. The r_c/D for these configurations is the same ($r_c/D = 1.38$), so that the dependence of the exit velocity profile on this nondimensional ratio is further indicated.

The data for constant-area transition bends with cross section changing from annular to circular (configurations 6, 7, and 8 in fig. 4(c)) indicate that the transition upstream from the bend produced somewhat less flow separation than the plain circular bend of configuration 1 (compare figs. 4(c) and 4(a)). Bends with cross-section transition produced more separation than the plain annular bend (configuration 2), because of the inability of the transition innerbody to control and turn the flow, and about the same amount of separation as the plain circular bend. Transition after the bend again produced the most uniform exit distribution with no evident separation.

Diffusing bends (configurations 9 and 10) are presented in figure 4(d). No significant differences are apparent in the exit velocity distributions of the two diffusing bends. A large region of stagnant air was evident at the exit station with the main mass flow of air between the bend center line and the outer wall. The annular bend (configuration 10) produced somewhat higher local total-pressure losses. The circular bend produced a static-pressure rise of 20 percent (table II) as compared with 10 percent for the annular expanding bend. The ideal static-pressure rise for these bends is 73 percent. Successful diffusing bends must have a much higher radius of curvature than that of the configurations investigated herein and possibly special wall contours to avoid the high adverse pressure gradients on the inner wall.

The reducing bends investigated (configurations 11 and 12) both have good exit velocity distributions (fig. 4(e)), although the velocity at the inner wall for the circular-cross-section reducing bend (configuration 11) is very low. This velocity defect would be eliminated by use of a slightly larger radius of turn or by addition of a longer duct at the exit. The data show that, if appreciable area reduction occurs in the bend, high performance can be obtained even with simple circular-arc wall shapes.

Surveys were made at the bend exit for several of the configurations to determine the effect of tufts on the velocity distribution. Originally, it was thought that tufts might act as a boundary-layer control and speed the momentum interchange between free-stream flow and the flow near the wall. For those configurations investigated, only two (configurations 3 and 6) indicated discrepancies in the exit velocity distributions measured with and without tufts. The velocity distributions measured with tufts installed for these two configurations are shown in figures 4(b) and 4(c) as dashed curves. The separated region along the inner wall at the exit station is increased by approximately 0.3 inch when tufts are added. None of the remaining exit velocity distributions measured with tufts in the bend exhibited any differences from those measured without tufts. The number of tufts does not appear to be responsible for changed velocity distributions. Configuration 6 had relatively few tufts but indicated a displacement of the separated region, whereas configuration 7 had appreciably more tufts but indicated no change in the velocity profiles. Photographs of these two configurations (6 and 7) are presented as figure 5.

Mean Total-Pressure-Loss Coefficients and Exit Total-Pressure Distortions

Bar graphs of the corrected mean loss coefficients and exit total-pressure distortions are given in figure 6 for each configuration. The results for configurations 1 and 2 permit a direct comparison of the performances of a circular bend and an annular bend for the case in which the radius ratio of the outer shell of the annulus is equal to the radius ratio of the circular bend. The annular bend produced a slightly higher loss than the circular bend due to the estimated added friction of the annulus; however, the annular bend produced considerably less total-pressure distortion than the circular bend due to the favorable effect of the inner body on the flow distribution, as previously discussed.

For the bends which had a transition from a circle to an annulus (configurations 3, 4, and 5) the configuration in which the transition occurred within the bend was the most compact arrangement and had about the best performance. Locating the transition downstream from the circular bend (configuration 5) produced a high total-pressure distortion due to the badly separated flow delivered by the circular bend to the transition duct. The data show that the leading edge of the center body should be located at or upstream from the bend inlet similar to configurations 3 and 4.

A comparison of the mean loss coefficients for configurations 1 and 5 shows that configuration 5 produced a higher loss coefficient than configuration 1 by an amount approximately equal to the friction losses

to be expected in the transition piece. Since the surveys of configuration 5 did not indicate separated flow, no mixing-loss correction was made; whereas, this correction was made to the data of configuration 1. The resulting loss coefficient of configuration 1 appears to be correct in magnitude when compared with that for configuration 5; therefore, the method used is considered to be satisfactory.

The data for bends with transitions from an annulus to a circle (configurations 6, 7, and 8) show that the case in which the transition occurred within the bend proper (configuration 7) produced the lowest loss coefficient; however, it also produced the highest total-pressure distortion. Terminating the center body at the bend exit apparently permitted the configuration to operate in very much the same manner as the plain circular bend except for some reduction in the total-pressure distortion. Locating the transition piece upstream from the bend produced a slightly higher loss than the basic circular bend (configuration 1) as would be expected, but the basic bend flow pattern was altered by the transition section to the extent of producing substantially less total-pressure distortion. Locating the transition duct downstream from the bend proper produced both a high loss and a high total-pressure distortion. These results are due to the substantial secondary flows generated on the downstream part of the center body and discharged into the mainstream at the terminus of the center body. The data suggest that an optimum design would be a compromise between configurations 6 and 7 with the center body terminated at some location within the bend.

The diffusing bends (configurations 9 and 10), which had an area ratio of 1.91, produced total-pressure losses of the order of twice the losses of comparable constant-area designs. The total-pressure distortions were correspondingly high. The performance of the annular-type expanding bend (configuration 10) was substantially worse than that of the circular bend, probably due to the development of secondary flows on the inner body.

The reducing bends (configurations 11 and 12), which had an area ratio of 0.523, produced somewhat less losses and considerably lower total-pressure distortions than the comparable constant-area designs. The transition from circle to annulus within the bend had a favorable effect on the distortion index in the case of configuration 12, as it had for configuration 4, in comparison with the values obtained for the corresponding circular bends without transitions.

CONCLUDING REMARKS

Circular and annular 90° bends of simple shapes were investigated for cases in which the cross-sectional area was constant, expanding, and contracting. Two series of transition bends (circular to annular and annular

to circular) were included in which the transition occurred upstream of the bend, within the bend, and downstream from the bend. The principal data taken were exit total- and static-pressure distributions. The following general observations are made:
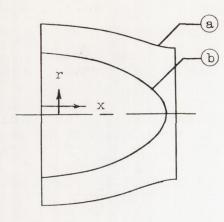
1. The constant-cross-section annular bend had slightly more loss than the corresponding constant-cross-section circular bend because of the higher friction loss of the annulus, but the annular bend produced a less distorted exit flow distribution than the circular bend. The results indicate that for bends of constant area and constant cross section, the flow distribution is a function of the ratio of the radius of curvature to the diameter of a circle with the same area as the cross-section flow area of the bend.

2. For the constant-area-bend configurations which included a transition from a circle to an annulus, the configurations in which the transition started at or upstream from the bend inlet produced the highest performance.

3. For the constant-area-bend configurations with transition from an annulus to a circle, the configuration in which the transition occurred upstream from the bend produced the least exit total-pressure distortion. The configuration in which the transition occurred within the bend produced the least total-pressure loss.

4. The performance of the two diffusing bends, which had an area ratio of 1.91, was extremely poor. The bend which included an annular to circular transition within the bend had a particularly low performance probably due to the development of secondary flows on the inner body.

5. The two reducing bends, which had an area ratio of 0.523, had somewhat less total-pressure losses and considerably lower total-pressure distortions than the comparable constant-area designs.

Langley Aeronautical Laboratory,
    National Advisory Committee for Aeronautics,
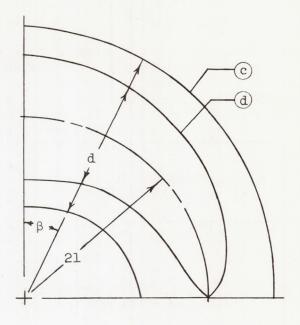   Langley Field, Va., February 1, 1957.

REFERENCES

1. Gray, S.: A Survey of Existing Information on the Flow in Bent Channels and the Losses Involved. Power Jets Rep. No. R. 1104, Power Jets (Res. and Dev.), Ltd., June 1945.

2. Henry, John R.: Design of Power-Plant Installations. Pressure-Loss Characteristics of Duct Components. NACA WR L-208, 1944. (Formerly NACA ARR L4F26.)

3. Higginbotham, James T., Wood, Charles C., and Valentine, E. Floyd: A Study of the High-Speed Performance Characteristics of 90° Bends in Circular Ducts. NACA TN 3696, 1956.

4. Wyatt, DeMarquis D.: Analysis of Errors Introduced by Several Methods of Weighting Nonuniform Duct Flows. NACA TN 3400, 1955.

5. Valentine, E. Floyd, and Copp, Martin R.: Investigation To Determine Effects of Rectangular Vortex Generators on the Static-Pressure Drop Through a 90° Circular Elbow. NACA RM L53G08, 1953.

6. Weske, John R.: Experimental Investigation of Velocity Distributions Downstream of Single Duct Bends. NACA TN 1471, 1948.

TABLE I.- ORDINATES OF BEND SECTIONS WITH
VARIABLE CURVATURE

x	r, in.	
	(a)	(b)
0	10.5	7.25
1	10.485	7.23
2	10.44	7.16
3	10.32	7.05
4	10.22	6.89
5	10.08	6.68
6	9.91	6.42
7	9.74	6.10
8	9.52	5.73
9	9.25	5.28
10	8.95	4.76
11	8.64	4.15
12	8.31	3.42
12.5	8.115	3.02
13	8.00	2.56
13.5	7.86	2.08
13.75	7.80	1.82
14	7.735	1.52
14.1	-----	1.37
14.2	7.695	1.20
14.3	-----	.99
14.4	7.655	.71
14.5	-----	0
14.6	7.625	----
14.8	7.60	----

β, deg	d, in.	
	(c)	(d)
0	21.0	14.5
10	20.76	14.13
20	20.10	13.15
30	19.45	11.95
40	18.76	10.80
50	18.06	9.66
60	17.36	8.38
70	16.66	6.84
80	15.92	4.84
82	-----	4.40
84	-----	3.81
86	-----	3.01
88	-----	1.84
90	15.19	-----

TABLE II.- CIRCUMFERENTIAL IMPACT-PRESSURE VARIATION AT INLET AND EXIT

Configuration	$\dfrac{q_{c,r}}{p_{t,r}}$	Inlet $\dfrac{p_{t,r} - p_{wall}}{q_{c,r}}$				Exit $\dfrac{p_{t,r} - p_{wall}}{q_{c,r}}$			
		Top	Inner	Bottom	Outer	Top	Inner	Bottom	Outer
1	0.022	0.943	1.405	0.959	0.693	1.405	1.932	1.143	0.977
2	.029	.956	1.384	.955	.705	1.240	1.800	1.019	.846
[a]3	.030	1.012	1.037	1.011	.940	1.236	1.690	.986	.840
[a]4	.030	.970	1.280	.990	.760	1.130	1.547	.936	.788
5	.030	.954	1.355	.944	.747	1.260	1.289	1.255	1.194
6	.024	1.037	1.003	1.010	.950	1.233	2.094	1.200	.912
7	.025	.960	1.360	.980	.700	1.346	1.762	1.312	1.024
8	.024	.941	1.420	.963	.676	1.370	1.250	1.370	1.245
9	.030	.987	1.221	.998	.794	.928	.972	.743	.613
10	.029	.986	1.294	.968	.752	1.064	1.096	.827	.679
11	.007	.968	1.384	.946	.702	3.840	4.960	3.750	2.970
[a]12	.011	.929	1.463	.934	.674	3.700	4.580	3.150	2.670

[a]These configurations have a stagnation region at the inlet due to the proximity of the inner body.
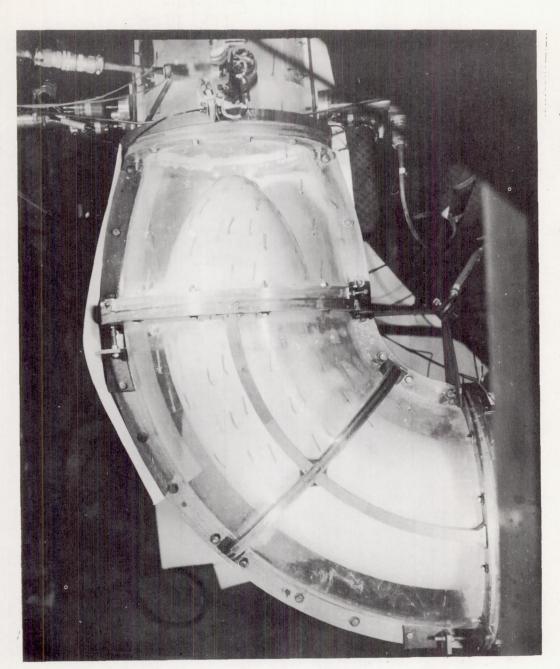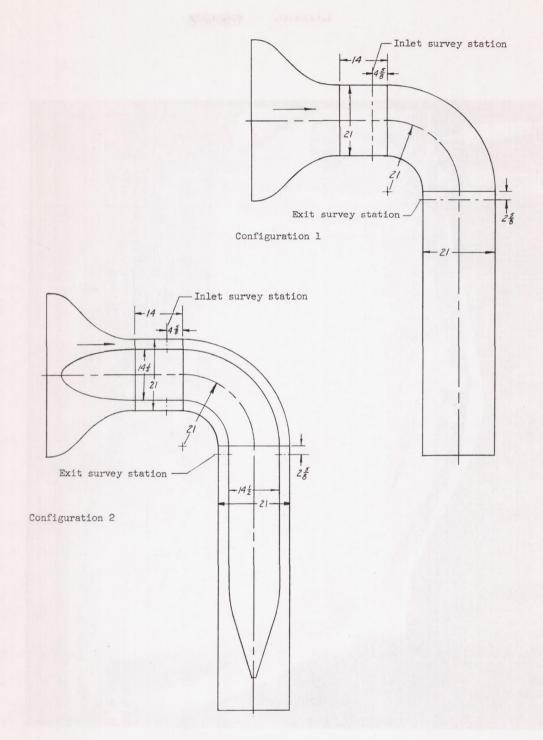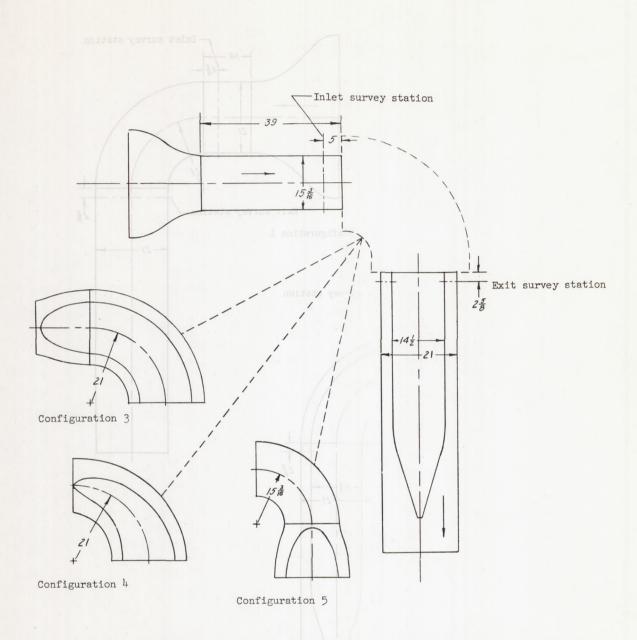
Figure 1.- Typical bend (configuration 8).   L-57-162

(a) Bends of constant cross section.

Figure 2.- Bend configurations investigated. All dimensions are in inches
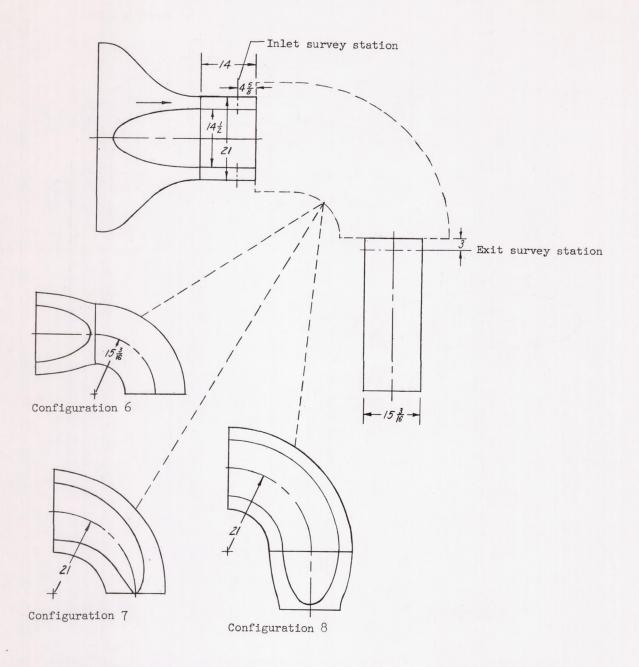unless otherwise indicated.

(b) Constant-area transition bends with cross section changing from cir-
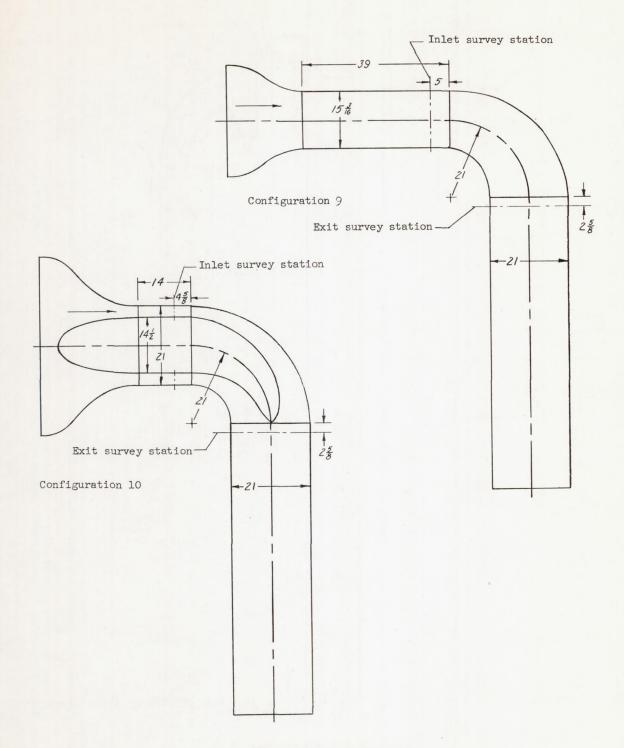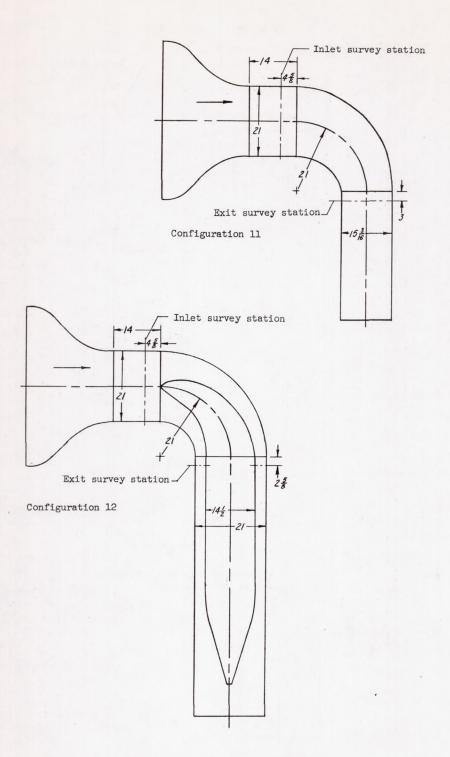cular to annular.

Figure 2.- Continued.

(c) Constant-area transition bends with cross section changing from annular to circular.
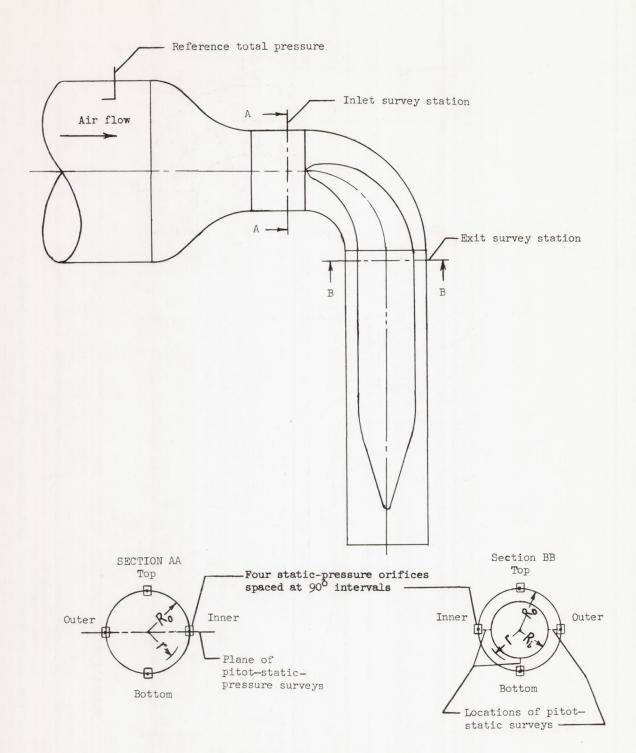
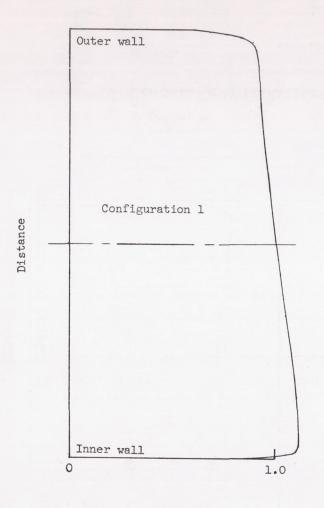Figure 2.- Continued.
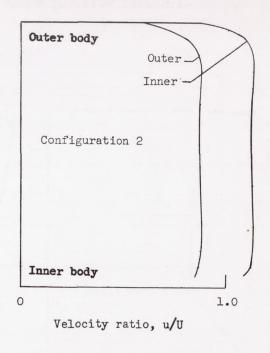
(d) Diffusing bends.

Figure 2.- Continued.

Configuration 11

Configuration 12

(e) Reducing bends.

Figure 2.- Continued.

Reference total pressure

Air flow

A

Inlet survey station

A

Exit survey station

B   B

SECTION AA
Top

Outer   Inner

R_O

r

Bottom

**Four static-pressure orifices
spaced at 90° intervals**

Plane of
pitot-static-
pressure surveys

Section BB
Top

Inner   Outer

R_O

r R_i

Bottom

Locations of pitot-
static surveys

(f) Typical instrumentation.

Figure 2.- Concluded.

Outer wall

Distance

Configuration 1

Inner wall

0   1.0

Velocity ratio, u/U

Outer body

Outer

Inner

Configuration 2

Inner body

0   1.0
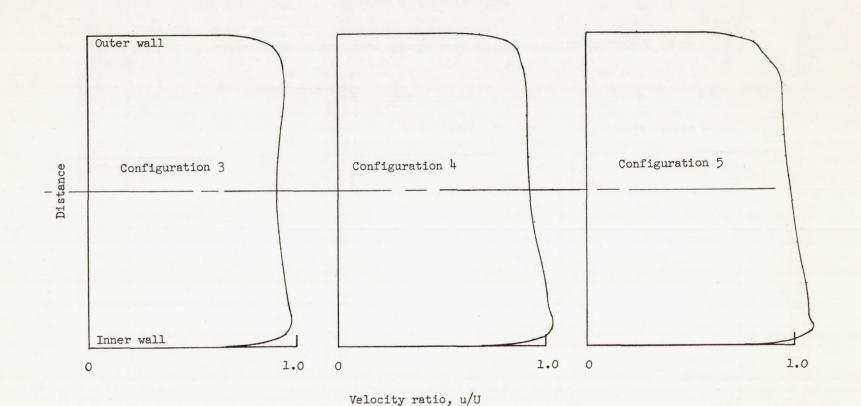
Velocity ratio, u/U

(a) Constant-cross-section bends.

Figure 3.- Inlet velocity distributions.
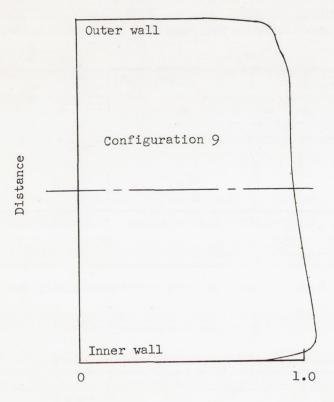
(b) Constant-area transition bends with cross section changing from circular to annular.

Figure 3.- Continued.

Distance

Outer body

Outer

Inner

Configuration 6

Inner body

0   1.0

Outer

Inner

Configuration 7

0   1.0

Outer

Inner

Configuration 8

0   1.0

Velocity ratio, u/U

(c) Constant-area transition bends with cross section changing from annular to circular.

Figure 3.- Continued.

Outer wall

Configuration 9

Distance

Inner wall

0   1.0

Outer body   Outer ─
                  Inner ─

Configuration 10

Inner body

0   1.0
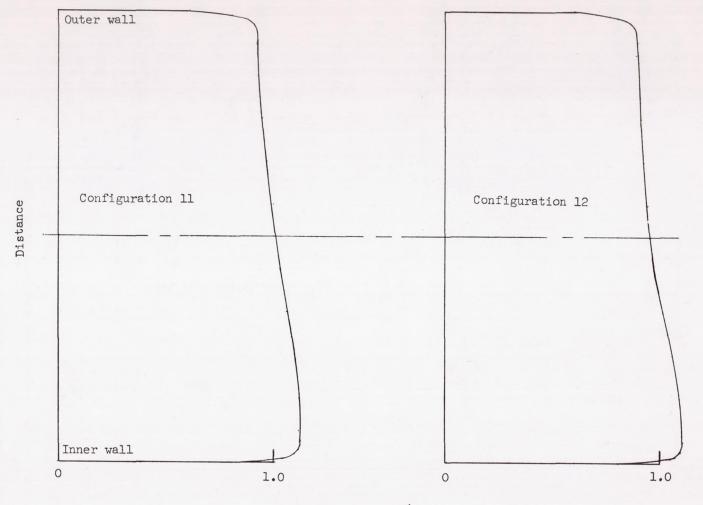
Velocity ratio, u/U

(d) Diffusing bends.

Figure 3.- Continued.

Outer wall

Configuration 11

Distance

Inner wall

Configuration 12

0   1.0   0   1.0
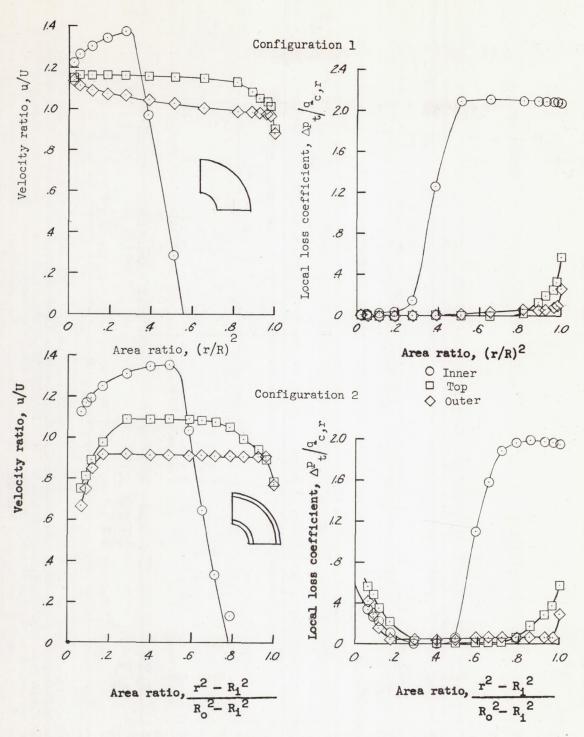
Velocity ratio, u/U
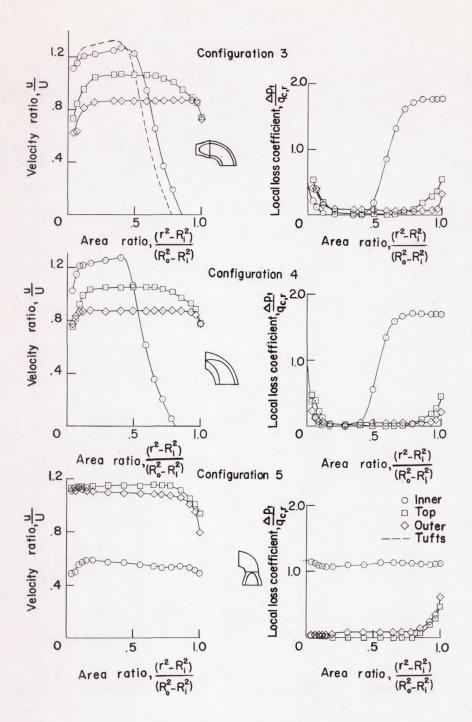
(e) Reducing bends.

Figure 3.- Concluded.
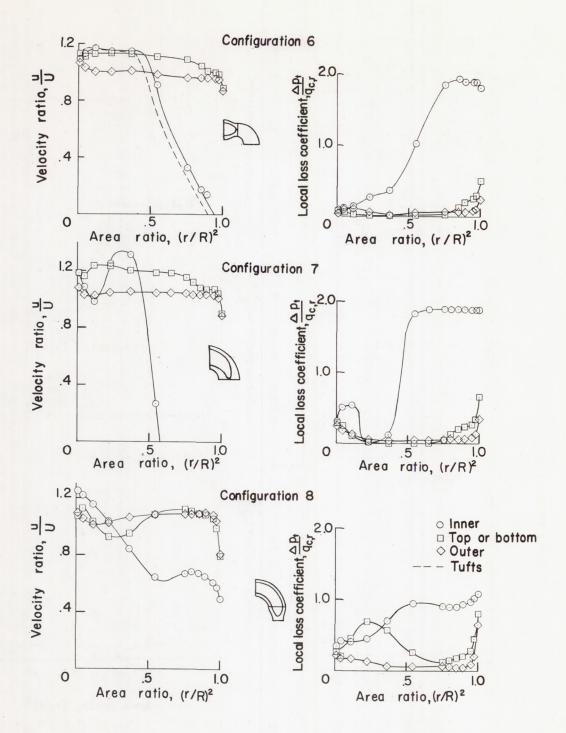
(a) Constant-cross-section bends.

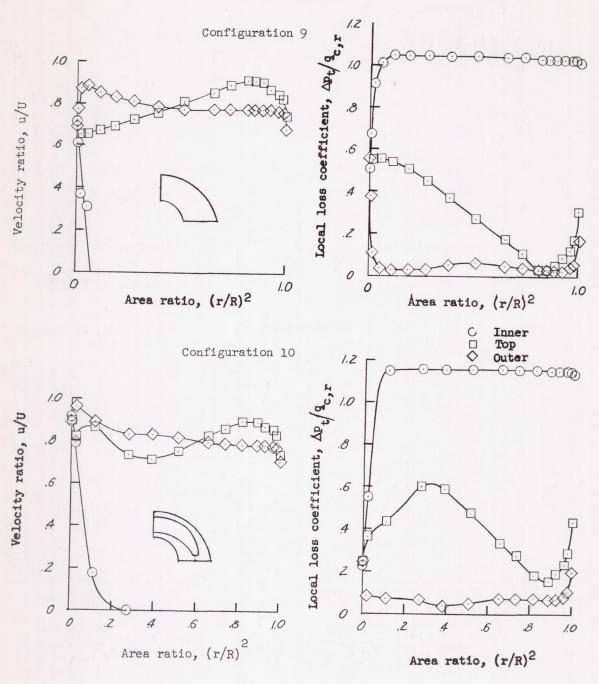Figure 4.- Exit velocity and total-pressure distributions.

(b) Constant-area transition bends with cross section changing from circular to annular.
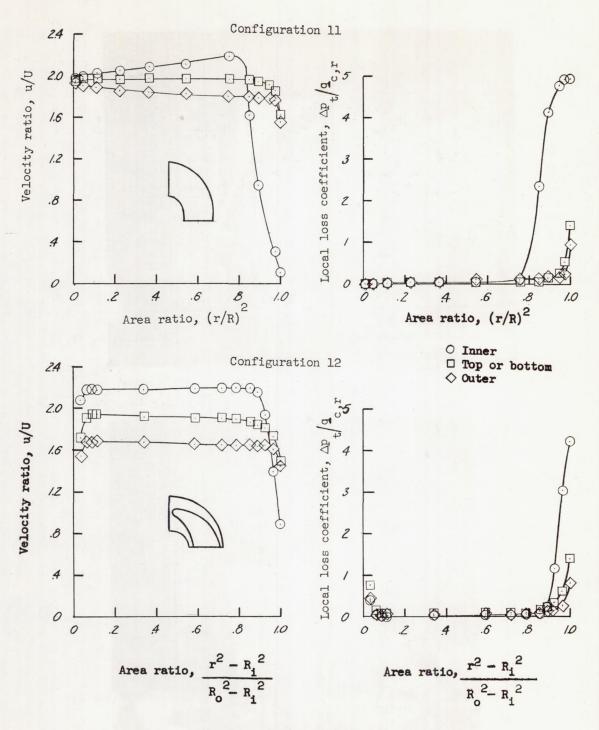
Figure 4.- Continued.

(c) Constant-area transition bends with cross section changing from annular to circular.
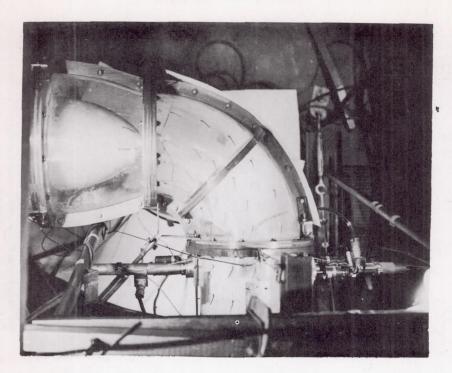
Figure 4.- Continued.

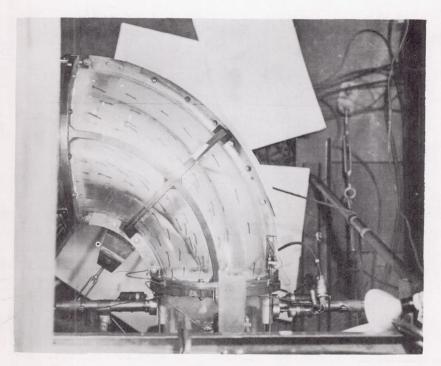(d) Diffusing bends.

Figure 4.- Continued.

Configuration 11

Configuration 12

○ Inner
□ Top or bottom
◇ Outer

(e) Reducing bends.

Figure 4.- Concluded.

Configuration 6

Configuration 7
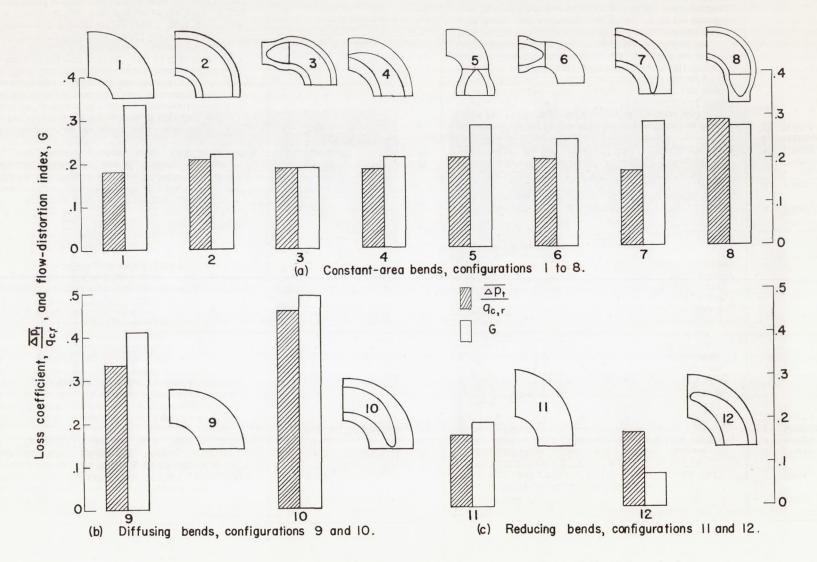
Figure 5.- Configurations 6 and 7 with tufts.   L-57-163

(a) Constant-area bends, configurations 1 to 8.

$\dfrac{\overline{\Delta p_t}}{q_{c,r}}$

G

(b) Diffusing bends, configurations 9 and 10.

(c) Reducing bends, configurations 11 and 12.

Loss coefficient, $\dfrac{\overline{\Delta p_t}}{q_{c,r}}$, and flow-distortion index, G

Figure 6.- Total-pressure-loss coefficient and flow-distortion index.